Research Article

Investigation on the Deterioration Mechanism of Recycled Plaster

Zhixin Li [iD],[1] Kaidong Xu,[1] Jiahui Peng,[2] Jina Wang,[1] Xianwei Ma [iD],[1] and Jishou Niu[1]

[1]*School of Material and Chemistry Engineering, Henan University of Urban Construction, Pingdingshan 467036, China*
[2]*College of Materials Science and Engineering, Chongqing University, Chongqing 400045, China*

Correspondence should be addressed to Zhixin Li; li.zhixin1989@163.com

The deterioration mechanism of recycled plaster (R-P) was studied. The large specific surface area (SSA), improper preparation temperature, increased water requirement of R-P, and microstructure of its hardened body were analyzed by particle size distribution (PSD), Blaine method, differential scanning calorimetry (DSC), scanning electron microscopy (SEM), and nitrogen adsorption porosimetry. The results indicated that the properties of R-P were deteriorated, but its strength decreases from 50% at the same manufacturing process to 30%–40% at similar specific surface area. The analysis shows that the large SSA, poor morphology, narrow PSD, and increased internal detects give rise to increase of water requirement. In addition, the deterioration properties are caused by unsuitable temperature of preparation, loose structure, and large average pore diameter in hardened R-P as well.

1. Introduction

The development of economy has brought about the wide use of plaster of Paris (POP) in construction [1–3] and in ceramic factories [4, 5] as the raw materials of slip casting models, thus producing brazen increase of waste gypsum (WG) after their utilization. According to Suárez, the output of gypsum wallboards produced annually is 80 million tons, and the amount of gypsum dumped in landfills is 15 million tons per year [6]. It not only wastes the gypsum resources but also arouses environment problems, endangering human health [7–9]. Hence, recycling WG is necessary for offering cost reduction and environment protection.

Great efforts have been exerted in the utilization of WG and several approaches are also tried, such as using WG as a retarder in making Portland cement [6], soft clay [10–13], ceramic products [14], new drywalls, and non-load-bearing bricks [15]. However, in most of the related application mentioned above, the utilization of WG is limited, and the problems brought by WG can not be effectively solved. Large plate gypsum is also prepared from WG via the wet process [16], which is unfavorable considering the complex process and may not be feasible in the industrial production on a large scale. β-Hemihydrate of calcined WG (R-P) as a low-energy material can be produced by the reversible reaction between gypsum dihydrate and gypsum hemihydrate in an electric oven at 180°C [16]. Nevertheless, the utilization is still very little owing to the deterioration performances of R-P compared with POP. So, mastering the deterioration mechanism of R-P is of great importance and urgency for its utilization. There have been several investigations on the deterioration mechanism of R-P, and the deterioration is commonly ascribed to its large specific surface area [17]. However, only limited research on other possible factors inducing R-P deterioration except for the large specific surface areas (SSAs) was published in the common sources by the scholars, which seriously hinders the utilization of R-P. Our study found that the unsuitable preparation temperature, increase of water requirement, and microstructure changes of its hardened R-P were also important factors. Thus, deterioration mechanism of R-P studied in our work is systematic.

In this paper, the above mentioned factors have been fully analyzed to investigate the deterioration mechanism of R-P comprehensively. The authors expect the research will lay a ground work for the utilization of R-P.

TABLE 1: Chemical composition of VG used (%).

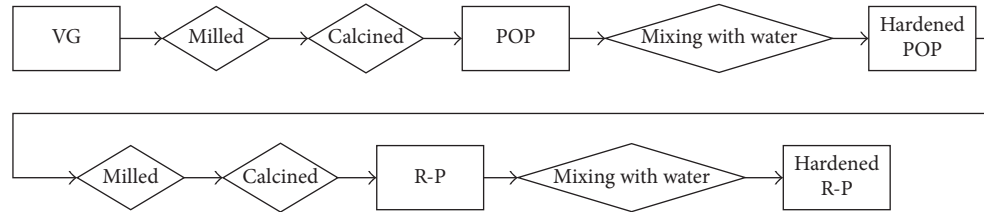| Virgin gypsum	SO_3	CaO	SiO_2	Al_2O_3	Fe_2O_3	K_2O	SrO
Chemical composition	47.57	38.73	1.15	0.42	0.13	0.07	0.04

FIGURE 1: The flowchart of preparing R-P and its hardened R-P.

TABLE 2: Properties of POP and R-P under the similar SSA.

Gypsum	SSA ($m^2 \cdot kg^{-1}$)	W/P	Setting time (min)		2 h strength (MPa)		Dry strength (MPa)		Water absorption (%)
			Initial	Final	Flexural strength	Compressive strength	Flexural strength	Compressive strength	
POP	1098	0.68	26	30	2.47	4.59	4.50	6.98	38.89
R-P	1114	0.85	33	46	1.66	2.94	2.70	4.80	40.65

2. Experimental Details

2.1. Materials and Preparation of R-P. The virgin gypsum (VG) was purchased from Yingcheng in China. The chemical composition of VG determined by X-ray fluorescence (XRF) is shown in Table 1. Preparation of R-P is shown in Figure 1, and their measurement of water-plaster ratio (W/P), setting time, and strength were done according to GB/T 9776-2008 [18]. The experimental details have been introduced in our earlier research [19], and the SSA was tested according to GB/T 8074-2008 [20].

2.2. Experimental Techniques. To eliminate the effect of SSA of R-P, it is necessary to mill POP into the approximate SSA with R-P (Table 2). Thus, POP with SSA of 1098 m^2/kg and R-P with SSA of 1114 m^2/kg were employed to analyze possible influencing factors that can induce the deterioration of R-P.

In order to study the effect of unsuitable preparation temperature on the deterioration of R-P, the relationship between strength and calcination temperatures was established. Moreover, the calcination temperatures are 130°C, 150°C, 160°C, 165°C, 170°C, 175°C, 180°C, and 200°C (Figure 2), respectively.

To facilitate understanding the going of the work, a diagram for experimental work is presented in Figure 3. Briefly, the properties (water requirement, setting time, strength, and water absorption) were measured first, and then the deterioration mechanism was determined from the large SSA, unsuitable preparation temperature, reasons for increased water requirement, and microstructure changes of its hardened R-P.

2.3. Materials Characterization. The morphological investigations were observed by the scanning electron microscope (TESCAN VEGA III LMH). The internal detects were measured via simultaneous DSC/TG instrument (SMP/PF7548/MET/400W) [21]. The particle size distribution was analyzed via a laser particle size analyzer (Mastersizer 2000) after dispersing POP and R-P in anhydrous ethanol with an ultrasonic bath. Pore size distribution and porosity of pastes were investigated by an adsorption meter (ASAP 2020) with nitrogen full adsorption.

3. Results and Discussions

3.1. Large Specific Surface Area. Under the same preparation process as POP, the properties of R-P were deteriorated seriously, which is displayed in Table 3. Clearly, the W/P {ml water/300 g plaster powder (water-plaster ratio)}, setting time, and water absorption were all increased, whereas the strength of R-P was decreased by approximately 50% (Figure 4). At this time, SSA of R-P was increased from 452 m^2/kg to 1114 m^2/kg; thus, the deterioration properties of R-P were caused by its large SSA, which is in harmony with the previous findings [17].

Table 2 gives the properties of R-P and POP under the similar SSA. This table was overwhelmingly proving that the properties of R-P were also deteriorated despite approximate SSA obtained by POP and R-P. To our surprise, the strength decreasing rate was reduced from 50% to 30%–40% (Figure 4). Therefore, it could be concluded that there were, in addition to large SSA brought about, other reasons for property deterioration of R-P.
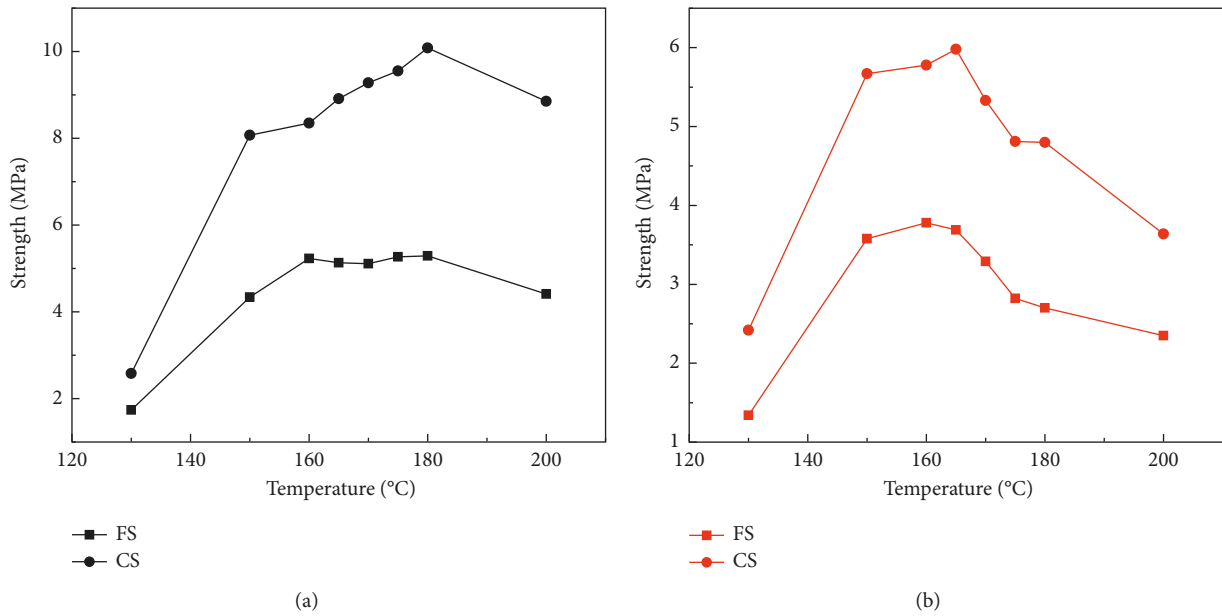
(a)

(b)

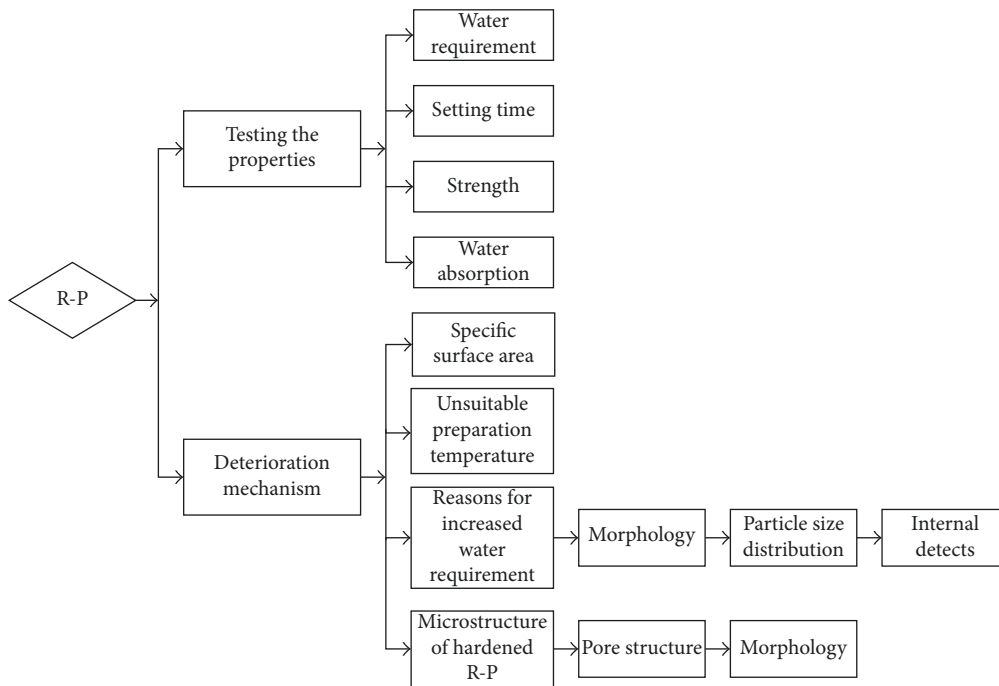FIGURE 2: Effect of preparation temperatures on the strength of POP and R-P.

FIGURE 3: The test program.

TABLE 3: Properties of POP and R-P under the same preparation process.

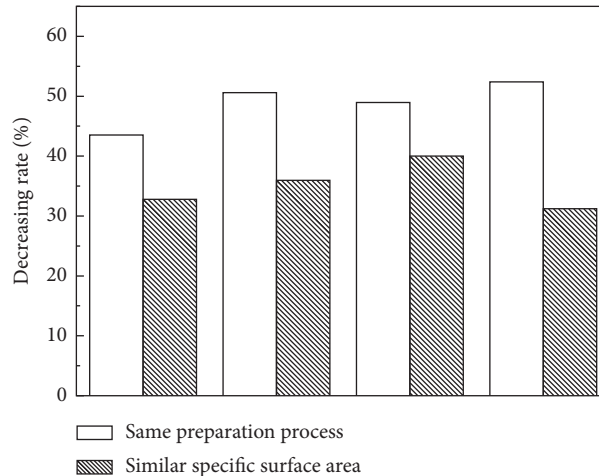| Gypsum	SSA ($m^2 \cdot kg^{-1}$)	W/P	Setting time (min)		2 h strength (MPa)		Dry strength (MPa)		Water absorption (%)
			Initial	Final	Flexural	Compressive	Flexural	Compressive	
POP	452	0.63	8.5	13.5	2.94	5.95	5.29	10.08	29.50
R-P	1114	0.85	33	46	1.66	2.94	2.70	4.80	40.65

Figure 4: The decreasing rate in the strength of R-P.

3.2. Unsuitable Preparation Temperature. It has been reported that under constant experimental conditions, gypsums of different origin have different dehydration characteristics and physical properties [22], and the reactivity of hemihydrate depends largely on the temperature of preparation [23]. So, we conclude that various physical properties of R-P can be observed under different calcination temperatures since it is known that strength is the comprehensive aspect charactering the properties of plaster. Therefore, an attempt has been made to correlate the strength of R-P and POP with different temperatures of preparation so as to find out the effect of preparation temperature on properties of R-P, which is seen in Figure 2.

As the preparation temperature increases, the strength changes of POP and R-P are shown in Figures 2(a) and 2(b), respectively. From the figures, it is clear that the compressive strength (CS) of POP increased rapidly to 10.08 MPa around 180°C and then dropped to 8.85 MPa at 200°C. The flexural strength (FS) of POP rose dramatically to 5.11 MPa around 160°C, and this number remained slightly increased until 180°C but then suffered a sharp drop. Therefore, the suitable preparation temperature of POP is 180°C; at this time, the initial setting time and final setting time are 8.5 min and 13.5 min, respectively, meeting the standard of GB 9776-2008 [18]. While for R-P, the compressive strength and flexural strength were at a peak around 165°C and 160°C, respectively. The setting time can satisfy the standard requirement when the calcination temperature was 165°C. Hence, it could be drawn that the unsuitable preparation temperature led to the deterioration properties of R-P as well.

3.3. Reasons for Increased Water Requirement. The morphology [24], particle size distribution (PSD) [25], and internal detects [21] are of critical factors associated with the water demand property of plaster. Hence, the morphology, PSD, and internal detects of POP and R-P were measured via SEM, laser particle size analyzer, and DSC curves, which are presented in Figure 5.

Figures 5(a) and 5(b) show the crystal morphology of POP and R-P, respectively. It can be seen that the morphology of R-P is totally different from that of POP, depending on their origin of gypsum. The morphology of plaster, made of needle-shaped gypsum crystals, changes with the properties of gypsum. The origin gypsum of POP was relatively dense with almost no pores (Figure 6(a)). However, the origin gypsum of R-P was loose with much pores (Figure 6(b)), which contributed to the morphology changes. Clearly, POP possesses many spheroidal particles and includes some rode-like crystals with an aspect ratio of 1-2. While the aspect ratio of R-P crystals increases, the morphology are changed to acicular-like crystals with an aspect ratio of 5-6, which make R-P crystals occupy acicular-like and rode-like crystals. According to the principle enunciated by Li et al. [19] and Peng et al. [24], the water requirement of plasters are increased with the increase of aspect ratio. The needle-shaped crystal has poor fluidity and can increase the water requirement of plaster greatly, and the ideal crystal has an aspect ratio of 1:1 for reducing the water demand. Hence, it can be concluded that the water requirement of R-P is increased by its poor crystals.

Simultaneously, particle size distribution (PSD) results presented in Figure 5(c) further confirm the increase of water demand of R-P. It is noticed that the grading of R-P is, though two peaks are both occupied, obviously different from POP. A broad peak of POP is observed, where the full width at half maximum (FWHM) of the first peak and second peak are 18.75 and 22.50, respectively, if the width of POP is 100. While a narrow peak is seen in R-P, FWHM of the first peak and second peak are 16.25 and 18.75, respectively. Besides, its average particle size of R-P decreases from 54.614 μm to 12.882 μm. The coarse plasters require little water while plasters with narrow PSD reduce the packing density, thus requiring much water for standard consistency [26]. Therefore, much water of R-P is acquired to satisfy the fluidity.

To gain further insight into the reasons for the increase of water requirement, DSC analysis was carried out to evaluate the internal detects of R-P, which is presented in
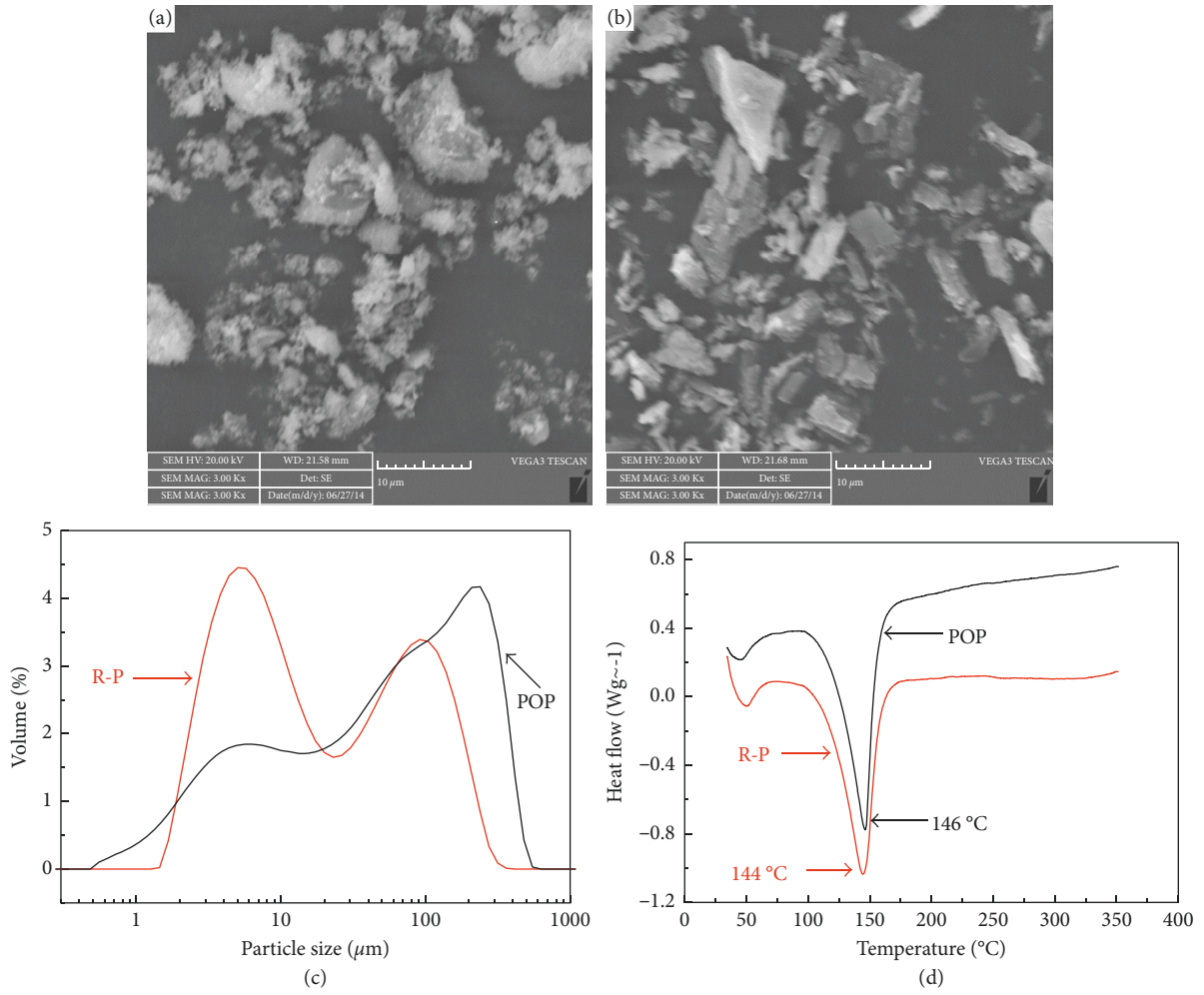
Figure 5: Microstructure, particle size distribution, and DSC curves of POP and R-P.
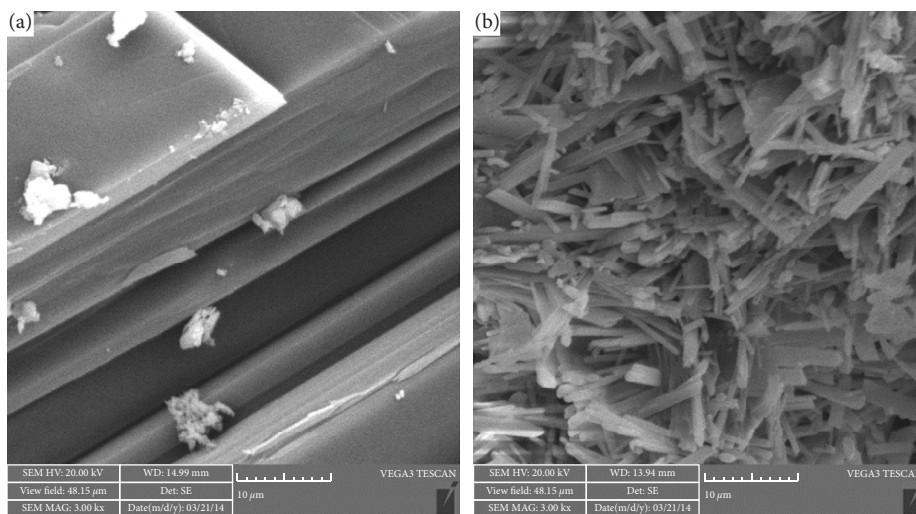

Figure 6: Microstructure of origin gypsum of POP and R-P.

Figure 5(d). Clearly, the decomposition temperature of R-P is 144°C, a little lower than that of POP. Some reported studies have indicated that plasters with little internal detects gain good crystallization while plasters with more internal detects have low decomposition temperature; thus, little internal detects acquire high decomposition temperature [21].
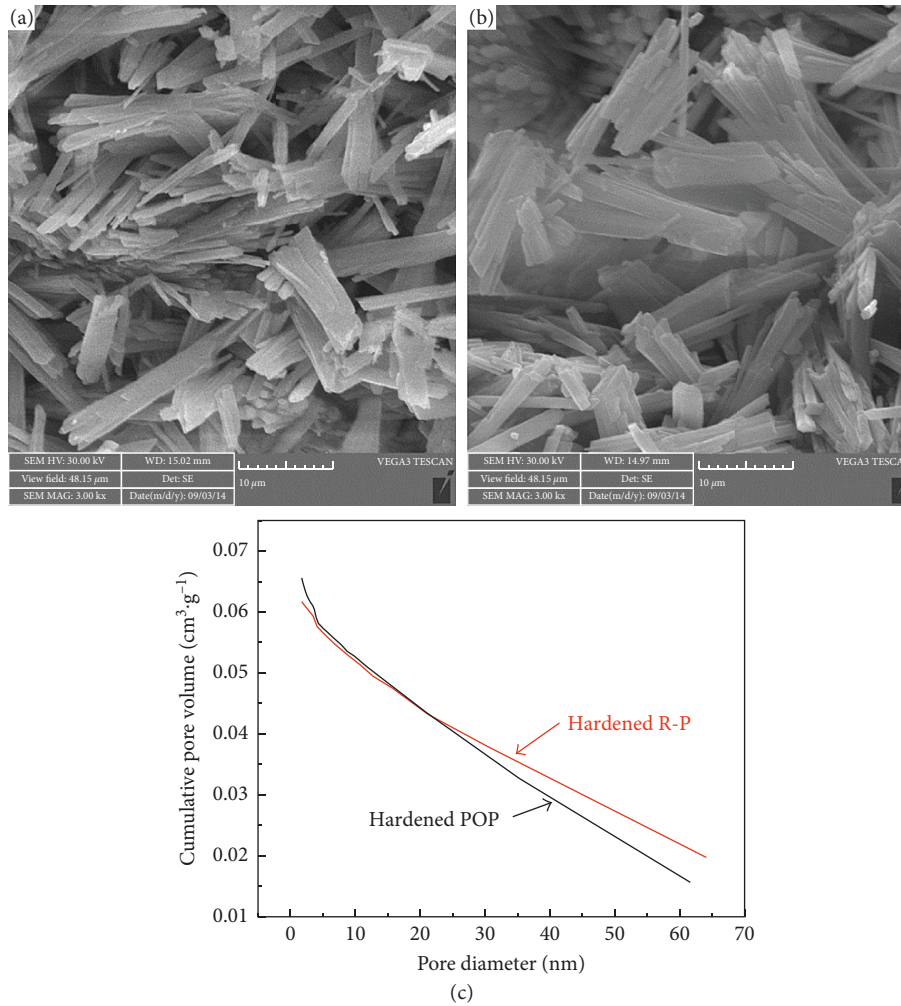
FIGURE 7: The morphology and pore size distribution of hardened POP and hardened R-P.

TABLE 4: Pore characteristics of hardened POP and hardened R-P.

Sample	Average pore diameter (nm)	Cumulative pore volume (cm$^3 \cdot$g^{-1})
Hardened POP	11.5892	0.066
Hardened R-P	14.6917	0.062

So, it could be concluded that more internal detects are obtained by R-P, increasing its water requirement, which is in good agreement with the SEM and PSD results.

Although the increased water requirement of R-P is not conducive for use in construction, it is of great importance for the ground improvement projects. According to Kamei et al., the improvement in strength when R-P was added to the soil was mainly depending on the potential of R-P to absorb water from the tested soil. The presence of R-P in soil mixture had a significant effect on the reduction of natural water content, subsequently the strength was improved.

3.4. Microstructure of Hardened R-P. The strength of R-P paste depends largely on the characteristics of the microstructure, such as crystal morphology and size, and characteristics of matrix joints and pore structure [25].

Therefore, the morphology and pore structure were measured by SEM and nitrogen adsorption porosimetry, respectively, which are shown in Figure 7 and Table 4.

The SEM images of hardened POP and hardened R-P are presented in Figures 7(a) and 7(b), where significant difference can be observed. Owing to the high W/P and low reaction rate, a loose structure with many tufted crystals was shown in hardened R-P. Crystals of short aspect ratio can be clearly observed as well, reducing the overlapping of crystals; consequently, the strength of R-P is weakened. While for hardened POP, the crystals are slightly refined, little rode-like crystals of short aspect ratio can be readily detected. It displays a relatively compacted network with much needle-like crystals of long aspect ratio interweaving together horizontally and vertically, resulting in the preferable development and lapping tightly of crystals attributing high strength of POP.

It is widely known that the characteristics of pore structure are of essential importance for understanding the strength and wettability of hardened R-P [23]. So the porosity and pore size distribution of hardened POP and hardened R-P are measured, which are displayed in Table 4 and Figure 7(c), respectively. Clearly, the average pore diameter of hardened R-P, though the close cumulative pore volumes with hardened POP are obtained, increases drastically. The high quantity of coarse pores existed in hardened R-P is also confirmed by the pore size distribution results in Figure 7(c). Fine pores acquire high strength while pores with big diameter obtain low strength. The pore structure results are good consistent with SEM. The attainment of low strength and high wettability is associated with its coarse pores. It is well known that wettability is an important parameter for construction. R-P presents high water absorption. Therefore, low moisture resistance would be observed under wet environment, and radical decrease of mechanical properties would appear with the increasing moisture as well, which limits its utilization in building construction.

4. Conclusions

The following conclusions can be drawn from this study:

(1) The properties of R-P are deteriorated; nevertheless, the strength decreases from 50% at the same manufacturing process to 30%–40% at similar specific surface area. Therefore, the large specific surface area contributes to the deterioration of R-P.

(2) Except for large specific surface area of R-P, there are other influencing factors increasing the water requirement, such as poor morphology, narrow particle size distribution, and its incremental internal detects.

(3) The suitable preparation temperature of R-P is reduced to 165°C; thus, the properties of R-P are deteriorated severely when unsuitable temperature of preparation is adopted.

(4) Hardened R-P possesses a loose structure and coarse pores, thus decreasing its strength.

(5) In principle, the research on recycled plaster will provide a theoretical basis of efficient utilization of waste gypsum.

Conflicts of Interest

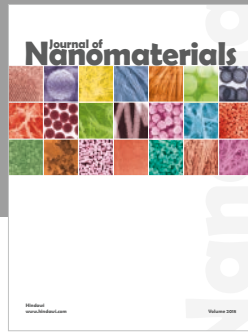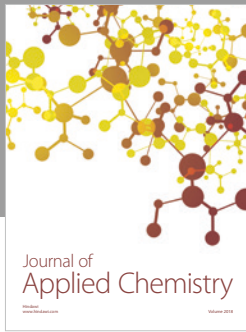The authors declare that they have no conflicts of interest.

Acknowledgments

References

[1] J. L. Davy, T. J. Phillips, and J. R. Pearse, "The damping of gypsum plaster board wooden stud cavity walls," *Applied Acoustics*, vol. 88, pp. 52–56, 2015.

[2] J. Zhou, Z. Shu, L. Tiantian, Y. Dongxue, Z. Sheng, and Y. Wang, "Novel fabrication route for non-fired ceramic tiles only using gypsum," *Ceramics International*, vol. 41, no. 7, pp. 9193–9198, 2015.

[3] J. Zhou, Z. Sheng, T. Li, Z. Shu, Y. Chen, and Y. Wang, "Preparation of hardened tiles from waste phosphogypsum by a new intermittent pressing hydration," *Ceramics International*, vol. 42, no. 6, pp. 7237–7245, 2016.

[4] H. C. Wu, Y. M. Xia, X. Y. Hu, and X. Liu, "Improvement on mechanical strength and water absorption of gypsum modeling material with synthetic polymers," *Ceramics International*, vol. 40, no. 9, pp. 14899–14906, 2014.

[5] N. B. Singh and B. Middendorf, "Calcium sulphate hemihydrate hydration leading to gypsum crystallization," *Progress in Crystal Growth and Characterization of Materials*, vol. 53, no. 1, pp. 57–77, 2007.

[6] S. Suárez, X. Roca, and S. Gasso, "Product-specific life cycle assessment of recycled gypsum as a replacement for natural gypsum in ordinary Portland cement: application to the Spanish context," *Journal of Cleaner Production*, vol. 117, pp. 150–159, 2016.

[7] O. Bergersen and K. Haarstad, "Treating landfill gas hydrogen sulphide with mineral wool waste (MWW) and rod mill waste (RMW)," *Waste Management*, vol. 34, no. 1, pp. 141–147, 2014.

[8] A. López and A. Lobo, "Emissions of C&D refuse in landfills: a European case," *Waste Management*, vol. 34, no. 8, pp. 1446–1454, 2014.

[9] T. Raghavendra and B. C. Udayashankar, "Engineering properties of controlled low strength materials using fly ash and waste gypsum wall boards," *Construction and Building Materials*, vol. 101, pp. 548–557, 2015.

[10] A. Ahmed, K. Ugai, and T. Kamei, "Investigation of recycled gypsum in conjunction with waste plastic trays for ground improvement," *Construction and Building Materials*, vol. 25, no. 1, pp. 208–217, 2011.

[11] A. Ahmed and K. Ugai, "Environmental effects on durability of soil stabilized with recycled gypsum," *Cold Regions Science and Technology*, vol. 66, no. 2-3, pp. 84–92, 2011.

[12] T. Kamei, A. Ahmed, and T. Shibi, "Effect of freeze–thaw cycles on durability and strength of very soft clay soil stabilised with recycled Bassanite," *Cold Regions Science and Technology*, vol. 82, no. 8, pp. 124–129, 2012.

[13] T. Kamei, A. Ahmed, and T. Shibi, "The use of recycled bassanite and coal ash to enhance the strength of very soft clay in dry and wet environmental conditions," *Construction and Building Materials*, vol. 38, pp. 224–235, 2013.

[14] A. P. Godinho-Castro, R. C. Testolin, L. Janke, A. X. R. Corrêa, and C. M. Radetski, "Incorporation of gypsum waste in ceramic block production: proposal for a minimal battery of tests to evaluate technical and environmental viability of this recycling process," *Waste Management*, vol. 32, no. 1, pp. 153–157, 2012.

[15] K. F. Ragab, *Recycling of Waste Gypsum Board to Produce New Drywalls and Non-Load Bearing Bricks*, American University in Cairo, Cairo, Egypt, 2014.

[16] Y. Kojima and T. Yasue, "Synthesis of large plate-like gypsum dihydrate from waste gypsum board," *Journal of the European Ceramic Society*, vol. 26, no. 4-5, pp. 777–783, 2006.

[17] L. N. Ren, *Reclaimed Gypsum Properties Change Law and Mechanism*, Standardization Administration of China, Beijing, China, 2014.

[18] GB/T 9776-2008, *Calcined Gypsum*, Standardization Administration of China, Beijing, China, 2008.

[19] Z. Li, J. Peng, and X. Qiu, "Effect of different ways of STPP retarder addition on properties of recycled gypsum," *Journal of Wuhan University of Technology*, vol. 32, no. 5, pp. 1125–1131, 2017.

[20] GB/T 8074-2008, *Testing Method for Specific Surface of Cement-Blaine Method*, Standardization Administration of China, Beijing, China, 2008.

[21] M. Guodong, "A study on the phase-transformation of the bassanites during hydration," *Journal of the Chinese Ceramic Society*, vol. 30, no. 4, pp. 532–536, 2002.

[22] R. A. Kuntze, "Differential thermal analysis of calcium sulphate dihydrate," *Nature*, vol. 193, no. 4817, pp. 429–432, 1962.

[23] M. J. Ridge and H. Surkevicius, "Influence of some conditions of calcination on the reactivity of calcium sulphate hemihydrate," *Journal of Chemistry Technology and Biotechnology*, vol. 12, no. 10, pp. 425–432, 1962.

[24] J. Peng, J. Qu, J. Zhang, C. Zou, and M. Chen, "Adsorption characteristics of EDTA on of α-hemihydrate desulfurization gypsum surface and its influence on crystal morphology," *Chinese Journal of Material Research*, vol. 25, no. 6, pp. 566–572, 2011.

[25] B. H. Guan, Q. Ye, Z. Wu, W. Lou, and L. Yang, "Analysis of the relationship between particle size distribution of α-calcium sulfate hemihydrate and compressive strength of set plaster—using grey model," *Powder Technology*, vol. 200, no. 3, pp. 136–143, 2010.

[26] Q. Ye, B. Guan, W. Lou, L. Yang, and B. Kong, "Effect of particle size distribution on the hydration and compressive strength development of α-calcium sulfate hemihydrate paste," *Powder Technology*, vol. 207, no. 1–3, pp. 208–214, 2011.